## ARTICLE IN PRESS

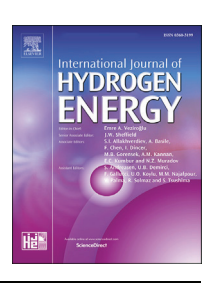
INTERNATIONAL JOURNAL OF HYDROGEN ENERGY XXX (XXXX) XXX



Available online at www.sciencedirect.com

## **ScienceDirect**

journal homepage: www.elsevier.com/locate/he



## Computational fluid dynamic modeling of methane-hydrogen mixture transportation in pipelines: Understanding the effects of pipe roughness, pipe diameter and pipe bends

Kun Tan, Devinder Mahajan, T.A. Venkatesh\*

Department of Materials Science and Chemical Engineering, Stony Brook University, Stony Brook, NY, USA, Institute of Gas Innovation and Technology, Stony Brook, NY, USA

#### HIGHLIGHTS

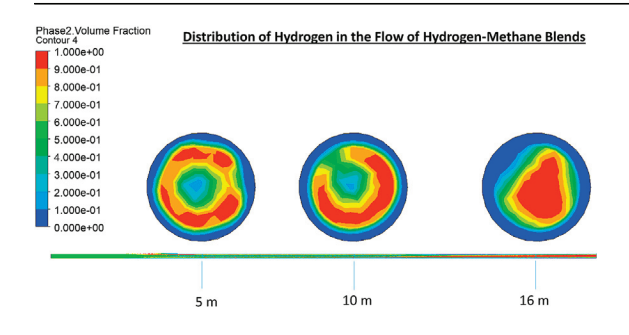
- Pipeline roughness increases transport energy requirements due to friction.
- Larger diameter pipelines transport hydrogen with more energy efficiency.
- Hydrogen content and flow conditions determine energy costs for transporting blends.
- Hydrogen gas blends develop coreannular flow pattern under steady state conditions.

## ARTICLE INFO

Article history:
Received 10 November 2022
Received in revised form
10 June 2023
Accepted 16 June 2023
Available online xxx

Keywords:
Hydrogen blending
CFD
Gas pipelines
Methane-hydrogen mixture
Energy transportation

#### GRAPHICAL ABSTRACT



#### ABSTRACT

A computational fluid dynamic modeling framework is developed to quantify frictional losses, assess the energy efficiency of transport, and characterize the mixing behavior of methane-hydrogen blends across representative regions of a large gas network such as transmission, distribution, and household pipeline sections. The principal conclusions from the present study are: (i) The increase in the energy required for transporting hydrogen as methane-hydrogen blends depends on the volume fraction of hydrogen, the nature of the flow conditions, pipe diameter, pipe roughness and pipe bends. (ii) Pipelines that have larger surface roughness or smaller diameters or those with bend sections require greater energy for transporting gas blends. (iii) The methane-hydrogen gas blends develop a core-annular flow pattern under steady state conditions with the denser and more viscous methane flowing near the pipe wall as the annulus while the less dense and less viscous hydrogen concentrated more towards the mid-sections of the pipelines.

© 2023 Hydrogen Energy Publications LLC. Published by Elsevier Ltd. All rights reserved.

0360-3199/© 2023 Hydrogen Energy Publications LLC. Published by Elsevier Ltd. All rights reserved.

<sup>\*</sup> Corresponding author. Department of Materials Science and Chemical Engineering Stony Brook University, NY 11794, USA. E-mail address: t.venkatesh@stonybrook.edu (T.A. Venkatesh). https://doi.org/10.1016/j.ijhydene.2023.06.195

#### Introduction

Hydrogen blending to the existing natural gas networks is considered as a reasonable intermediate step for achieving carbon neutrality and for enhancing the hydrogen economy. Some of the immediate benefits of hydrogen blending in existing natural gas networks include (i) adding calorific value to the existing energy supply using hydrogen produced from wind, solar, hydro, and other renewable energy sources; (ii) reducing greenhouse gas emissions for heat and electricity generation, while lowering other pollutants in selective engines; (iii) serving as a hydrogen delivery method to remote locations; (iv) inhibiting hydrate formation in subsea pipelines [1-5]. Projects around the world such as HyDeploy, GRHYD, THyGA, and Hyblend have assessed the impacts and implications of hydrogen blending to the existing natural gas networks, storage, and end-user applications [6-10]. Some of the technologies associated with hydrogen blending have been analyzed in laboratory scale and pilot scale experiments, as well as in numerical models and simulations.

Methane-hydrogen gas blends exhibit physical properties and combustion characteristics that are different from their constituents, i.e., pure methane or pure hydrogen. The density of methane-hydrogen mixture is lower than that of pure methane, which increases the gas leakage volumetric flow rate in pipes [11]. A significant reduction in viscosity occurs when the hydrogen volume concentration is greater than 50% in methane-hydrogen mixtures [12–14]. The lower heating values (LHV) of methane-hydrogen mixture increase slightly as more hydrogen content is introduced to the mixture. However, the LHV values of pure hydrogen are more than two times higher than any methane-hydrogen mixture with up to 90% hydrogen [15]. These property differences in the methane-hydrogen mixtures influence the flow behavior and the energy transport efficiency in pipeline transportation.

The feasibility of hydrogen blended methane as a fuel has been tested in a wide selection of end-user applications. Glanville et al. [16] tested three types of burners operating with 0-30% hydrogen blended methane-hydrogen mixtures. No flashback, flame life, and excessive CO emissions were found in the burners, while the overall burner efficiency changed about 1-1.5%. Zhao et al. [17] tested hydrogen injected natural gas in a commercial oven burner and found 25 vol% hydrogen addition to natural gas has no significant impact. Above 25% hydrogen content, the burner tube flashback became the limiting factor. A gas turbine engine originally designed for running natural gas was fueled with 0-90% hydrogen blended methane-hydrogen mixture in Shih and Liu's experiment [18]. Their study found that at low hydrogen content, addition of hydrogen in the fuel raises the flame temperature, which is favorable for the combustion efficiency. However, as the hydrogen concentration increases, the flame temperature drops and causes engine power shortage. This is largely due to a reduction in the mass flow rate of the fuel when methane is replaced by hydrogen. Under constant fuel flow rate conditions, increasing hydrogen concentration in the fuel elevates the flame temperature and combustor exit temperature and increases NOx emission, while under

constant energy flow conditions, increased CO emissions were detected. Wagner et al. [19] tested methane-hydrogen mixtures in a novel Gortex-based electrodes layered with Pd/ Pt catalysts fuel cell. Their study found no significant difference between pure hydrogen and 5% hydrogen injection in methane as a fuel. It was determined that diluted hydrogen fuel was as energy efficient as pure hydrogen, while methane acted as an inert carrier gas.

The effects of hydrogen injection in natural gas networks have also been investigated in prior studies. Bainier et al. [20] in their experiments, found that a lower energy quantity is transported as the volume percentage of hydrogen increases in the methane-hydrogen mixture. Thus, more compressor stations are required for pushing the gas mixture in the network. Quintino et al. [21] from a one-dimensional Cantera simulation, demonstrated that hydrogen with volume fractions up to 20% are fit for the existing natural gas infrastructure with minor technical modifications. Polyethylene (PE) pipelines are required in order to reduce hydrogen leakage when hydrogen content is above 30%. Additional compression stations are necessary to increase the pipeline pressure if hydrogen is added to the transmission lines. Hafsi et al. [22] modeled a close loop methane-hydrogen gas pipeline network and also suggested additional compressor stations were required to pay the compensation of pressure loss when hydrogen was blended to natural gas. Liu et al. [23] studied the effect of hydrogen injection in an existing natural gas network using a 1-D gas mixture model. As the hydrogen concentration increased, overpressure occurred when no change was made to the pressure stations. When the hydrogen concentration was greater than 30%, the transportation process became unstable, and the pipeline efficiency was reduced. Cavana et al. [24] examined the gas quality of a methane-hydrogen pipeline system and found hydrogen blending reduced both relative density and heating values of the gas mixture. Similar reduction in relative density and heating values have also been found in other numerical and experimental studies [25,26].

Umuteme [27] built a 2D computational fluid dynamics (CFD) model to study hydrogen injection into natural gas in a horizontal pipe. Their study found a reduction of downstream temperature with an increase in hydrogen gas volume concentration. Furthermore, it was observed that the force exerted on the inner wall was reduced as the volume of hydrogen injection increased. Liu et al. [28] built a CFD model to predict the decompression wave speed, which influenced the facture failure of pipe materials. They considered several equations of state in their CFD models and identified modeling conditions that provided best agreement with experimental results. They found that the variation of hydrogen concentration had a limited effect on the decompression wave speed when the hydrogen concentration was between 0 and 10% while a larger influence on the decompression wave speed was predicted in cases where the hydrogen concentrations were greater than 10%. Kuczynski et al. [29] studied pure methane and hydrogen-methane mixture in a pipeline flow simulation. The study found that 15% hydrogen reduces the outlet pressure by 10% compared to outlet pressure of the pure methane case. Furthermore, they also noted that the hydrogen content in a mixture of methane caused significant changes in natural gas pipeline thermodynamic transport conditions. Sulaiman et al. [30] evaluated the explosion severity of methane-hydrogenair mixture in a 90° pipe elbow using CFD. The results of the CFD models showed that both the bending geometry and the thermal diffusivity influenced the explosion severity. Lowering the hydrogen concentration in the mixture, reduced diffusivity, which led to decreased burning rate and flame speed. In addition to methene-hydrogen mixture transport in pipelines, dispersion process of methane and hydrogen was studied in CFD models as well. Wilkening and Baraldi [31] built pipeline gas leakage models for both methane and hydrogen under the same environment and flow conditions. Due to the lower density and higher sonic speed of hydrogen at the release, clouds of hydrogen gas traveled farther from the pipeline ground level, which decreased the ignition chance and reduced flame acceleration.

Cadorin et al. [32] analyzed high pressure gas flow through a pipe with CFD models using ANSYS CFX. Their study evaluated the energy transport efficiency of natural gas, biogas in two different compositions, and methanehydrogen mixtures. Their study found that a 10 vol % hydrogen methane-hydrogen mixtures in high Reynolds number flow conditions, self-consumes almost two times more energy than natural gas during transportation. Thus, more energy is required for transporting methane-hydrogen gas blends. Tan et al. [33] also developed CFD models to quantify the energy transport efficiency of a straight pipe section transporting methane-hydrogen mixture and to systematically assess the effects of hydrogen concentration and flow boundary conditions on the blended gas flow characteristics such as pressure drops. Their study demonstrated that the amount of increase in energy costs associated with the transport of hydrogen blends depends on the volume fraction of hydrogen and the nature of the flow conditions. The lowest energy costs are projected for transporting pure hydrogen under the conditions where the inlet velocity flow rates are similar to that used for transporting pure methane while the highest energy costs are expected when hydrogen is transported at the same mass flow rate as methane. However, a detailed study of the cost of transporting methane-hydrogen gas blends across various parts of the pipeline infrastructure such as transmission, distribution and household pipelines that takes into consideration the variations of pipe surface roughness and the effects of pipe bends is not yet available.

Prior studies have focused on understanding the mixing behavior of gases as well. Tichacek et al. [34] have suggested that in the laminar flow domain, axial mixing is the dominant mixing mechanism observed while in the turbulent flow domain, radial diffusion is the dominant factor that influences the mixing behavior. According to Dimotakis [35], turbulent mixing can be categorized into three levels. In level 1, passive scalar mixing, gases are usually density matched and the mixing does not couple back on the flow dynamics. In level 2, turbulent mixing is coupled to the flow dynamics, and additional external movement, such as an acceleration or gravitational field, is required. Finally, in level 3, turbulent mixing is

associated with changes in the fluid composition, density, enthalpy conversion, or pressure increase. An example of level 3 mixing can be found in combustion. Overall, it has been recognized that turbulent flows do not necessarily mix the transporting gas species unless some specific operating conditions are met. In fact, Buaria et al. [36] revealed that turbulence is an ineffective mixer when the Schmidt numbers are large for mixing passive scalars in turbulent flows. While some general insights have been obtained on the mixing behavior of gases, specific characteristics of the mixing behavior of hydrogen in methane gas blends have not been investigated in detail.

Hence, the objectives of the present study are.

- 1. To develop CFD models to capture the representative flow behavior of methane-hydrogen gas blends in transmission, distribution, and household pipelines.
- To characterize the pressure loss and energy costs associated with the transport of methane-hydrogen gas blends in pipelines with varying surface roughness, pipe diameter and pipe bends.
- To understand the influence of the differences in physical properties of methane and hydrogen on the mixing characteristics of methane-hydrogen gas blends in the pipelines.

## CFD modeling of methane-hydrogen gas blends

#### Governing equations

ANSYS FLUENT is the modeling software utilized in this study to simulate the methane-hydrogen mixture transportation in a pipeline section. The conservation of mass and momentum equations used in all CFD software are derivations of the Navier-Stokes equations. The conservation of mass or continuity equation of FLUENT (ANSYS FLUENT Theory Guide) is based on Equation (1).

$$\frac{\partial \rho}{\partial t} + \nabla \cdot (\rho \overrightarrow{\upsilon}) = S_m \tag{1}$$

In equation (1), the term  $\rho$  represents density, while v is the velocity vector.  $S_m$  is the source term, representing additional mass to the continuous phase, for example from phase transformation, or other sources defined by users.

A volume of fraction (VOF) model is used to describe the behavior of the methane-hydrogen mixture in the system. The advantage of the VOF model is that it only requires one set of momentum equations with tracking of volumetric fraction of each fluid in the flow domain to model a system of multiple immiscible fluids. In a VOF model, where multiple phases coexist in the system, the qth phase continuity equation can be expressed as given in Equation (2).

$$\frac{1}{\rho_1} \left[ \frac{\partial}{\partial t} (\alpha_q \rho_q) + \nabla \cdot \left( \alpha_q \rho_q \overrightarrow{v}_q \right) = S_{\alpha_q} + \sum_{p=1}^n (\dot{m}_{pq} - \dot{m}_{qp}) \right]$$
(2)

The term  $\alpha_q$  represents the volume fraction of the qth phase. The mass transfer from phase q to phase p is expressed

in the term  $\dot{m}_{qp}$ . The source term, S, can be defined for each phase. The conservation of momentum equation is listed below in Equation (3).

$$\frac{\partial}{\partial t}(\rho \overrightarrow{v}) + \nabla \cdot (\rho \overrightarrow{v} \overrightarrow{v}) = -\nabla p + \nabla \cdot (\overline{\tau}) + \rho \overrightarrow{g} + \overrightarrow{F}$$
(3)

The term p represents the static pressure. Gravitational forces and external forces are considered by  $\rho \vec{g}$  and  $\vec{F} \cdot \bar{\tau}$  is the stress tensor explained in Equation (4).

$$\bar{\tau} = \mu \left[ (\nabla \vec{v} + \nabla \vec{v}^{T}) - \frac{2}{3} \nabla \cdot \vec{v} I \right]$$
 (4)

The term  $\mu$  represents the molecular viscosity, while I is the unit tensor, and T represents temperature.

The transport equations for the standard k- $\epsilon$  model are presented in the equations below, in which k represents the turbulence kinetic energy, while  $\epsilon$  is the rate of dissipation. The term  $G_k$  represents the generation of turbulence kinetic energy due to mean velocity gradients. The term  $G_b$  represents the generation of turbulence kinetic energy due to buoyancy.  $Y_M$  is the contribution of the fluctuating dilatation in compressible turbulence to the overall dissipation rate. All constants are included as term G. The terms  $G_k$  and  $G_\epsilon$  are the turbulent Prandtl numbers. Lastly, the user-defined source terms are included as term G.

$$\frac{\partial}{\partial t}(\rho k) + \frac{\partial}{\partial x_{i}}(\rho k u_{i}) = \frac{\partial}{\partial x_{j}} \left[ \left( \mu + \frac{\mu_{t}}{\sigma_{k}} \right) \frac{\partial k}{\partial x_{j}} \right] + G_{k} + G_{b} - \rho \epsilon - Y_{M} + S_{k}$$
 (5

$$\begin{split} &\frac{\partial}{\partial t}(\rho\epsilon) + \frac{\partial}{\partial x_{i}}(\rho\epsilon u_{i}) = \frac{\partial}{\partial x_{j}}\left[\left(\mu + \frac{\mu_{i}}{\sigma_{\epsilon}}\right)\frac{\partial\epsilon}{\partial x_{j}}\right] + C_{1\epsilon}\frac{\epsilon}{k}(G_{k} + C_{3\epsilon}G_{b}) - C_{2\epsilon}\rho\frac{\epsilon^{2}}{k} \\ &+ S_{\epsilon} \end{split} \tag{6}$$

The Redlich-Kwong EOS was selected for simulating the gas mixture properties in the models because Cadorin et al. found that the Redlich-Kwong EOS provides a very good estimation of the fluid density and dynamic viscosity [32]. These two properties along with other physical properties of hydrogen and methane can be defined using the Redlich-Kwong EOS in FLUENT.

## CFD model for characterizing pressure drops and energy costs

A CFD model that predicts the flow behavior of a hydrogenmethane blend with 10 vol % hydrogen was constructed and validated [33]. The input properties of methane and hydrogen used in the CFD models such as density and viscosity are provided in Table 1. The geometry of the reference model was a 6 m cylindrical pipe with an inner diameter (ID) of 150 mm (Fig. 1). The mass flow rate of the transporting gas mixture in the pipe was 32.6 kg/s, which generated a turbulent flow. The value of sand grain roughness (ks=142 μm) was used to define the inner surface roughness of pipes. It was based on Schlichting's equivalent sand grain roughness model in which any rough surface geometry can be viewed as different size of sands glued to the surface [37]. The initial gauge pressure of the system was 6000 kPa, and the operating temperature was 303.15 K. A total of 476,965 mesh elements with average element size of 12 mm were utilized to build the geometry. Inflation was used to refine the near wall region of the mesh. A total of 7 inflation layers were included in the meshed geometry and total inflation layer thickness was 25 mm.

The pressure drop results were taken from the last 4 m of the pipe to avoid the unestablished flow domain near the inlet section. Fig. 1c and d illustrate the velocity and pressure results of the 6 m pipe model. It can be observed in the velocity contours, that the velocity profile near the inlet is a bit less uniform than the rest of the pipe. In the pressure contours, the overall pressure in the pipe is gradually reduced, moving from 6000 kPa at the inlet to 5960 kPa near the outlet. The last 4-m section of the pipe away from the outlet is a fair representation of the developed gas flow pattern. For the pipe geometry, fluid properties and flow conditions considered in this study, the variation of the pressure drop with flow distance appears to be largely linear over the 4 m section as well as in a longer 16 m section.

A mesh density study was also conducted to assess the influence of mesh density on the results obtained by the CFD models. Models with coarse and finer meshes (i.e., with 294,266 and 1024828 elements, respectively) were also developed. Compared to the models with lower mesh density, the

Table 1- Characteristics properties of methane, hydrogen and methane-hydrogen blends used as inputs for a set of CFD models and the outputs obtained from those CFD models.

			Methane/Hydrogen Vol. % Ratio				
		100/0	90/10	75/25	50/50	25/75	0/100
ṁ	[kg/s]	32.6	32.6	32.6	32.6	32.6	32.6
p	[kPa]	6000	6000	6000	6000	6000	6000
T	[K]	303.15	303.15	303.15	303.15	303.15	303.15
ρ	[kg/m³]	42.1	38.5	30.8	24.5	14.1	4.58
μ	[Pa s]	$1.26\times10^{-5}$	$1.22\times10^{-5}$	$1.15 \times 10^{-5}$	$1.10 \times 10^{-5}$	$1.00\times10^{-5}$	$9.15 \times 10^{-6}$
LHV	[KJ/kg]	50,050	50,910	52,673	57,442	68,845	119,900
Re	[-]	$2.20 \times 10^{7}$	$2.31\times10^{7}$	$2.34\times10^7$	$2.79 \times 10^{7}$	$2.99 \times 10^{7}$	$2.95 \times 10^{7}$
Δp	[kPa]	21.0	22.3	30.9	59.8	149.8	215.8
L	[m]	4	4	4	4	4	4
$f_N$	[-]	$1.95 \times 10^{-2}$	$1.89 \times 10^{-2}$	$2.10\times10^{-2}$	$3.23\times10^{-2}$	$4.65\times10^{-2}$	$2.18\times10^{-2}$
EST	$[m^{-1}]$	$2.50\times10^{-6}$	$2.84\times10^{-6}$	$4.76 \times 10^{-6}$	$1.06\times10^{-5}$	$3.86\times10^{-5}$	$9.82 \times 10^{-5}$

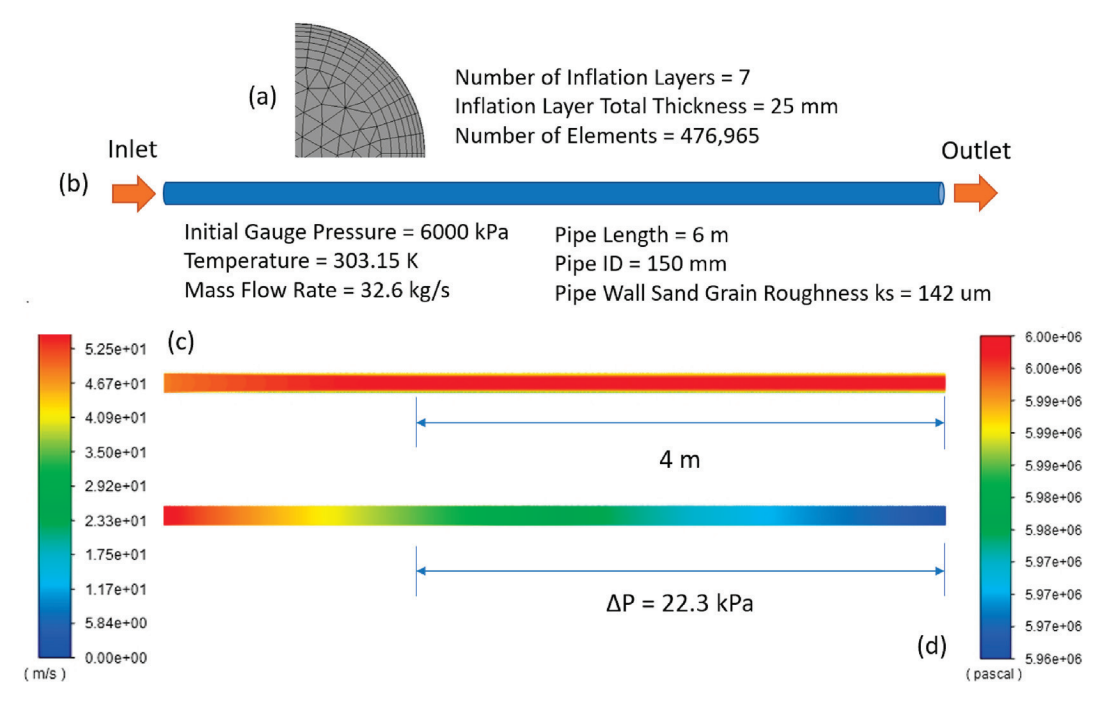


Fig. 1 — Details of the CFD model. (a) Mesh diagram; (b) Geometry and boundary conditions; (c) Velocity contours; (d) Pressure contours.

models with intermediate mesh density (i.e., 476,965 elements) provided a very close match with the results presented in Cadorin et al. [32]. Increasing the mesh density increased the computational time but did not result in a significant change in the results. Thus, it was determined that the intermediate mesh density models were adequate for the present study.

The expressions used to calculate the numerical friction factor ( $f_N$ ) and the energy specific toll (EST) are presented in Equations (7) and (8) [32]. In Equation (7),  $p_1$  and  $p_2$  represent the pressure at measuring point 1 and 2, respectively. The term A is the pipe cross section area, while  $\Delta x$  is equivalent to the length L in Equation (8).

$$f_{\rm N} = \frac{2(p_1 - p_2)D}{\rho \Delta x V_1^2} = -2\rho D \frac{\Delta p}{\Delta x} \frac{A^2}{m^2}$$
 (7)

$$EST = \frac{(\Delta p/\rho)}{LHV} \cdot \frac{1}{L}$$
 (8)

The energy specific toll (EST) provides a measure of the energy required to transport a fuel gas to offset pressure drops ( $\Delta p$ ), relative to its inherent energy (i.e., LHV), per unit length of a pipeline. (D=pipe diameter,  $V_1$ =inlet velocity,  $\dot{m}$ =mass flow rate,  $\rho$ =density of gas and L=length of pipeline.) Higher EST value would indicate that a greater amount of energy is required for transportation.

The results of the CFD model were validated by the Darcy-Weisbach equations applying different Moody frictional factors. In a previous study by Cadorin et al. [32], the effect of various mesh types, densities and models were studied extensively. After comparing to experiments (with natural gas), they found that k- $\epsilon$  model worked very well for the high velocity conditions in the pipe as well. So, they used the k- $\epsilon$  model for modeling a methane-hydrogen blend with 10 vol%

hydrogen as well. Hence, the k-  $\epsilon$  model has been adopted in this study to model the flow characteristics of methane-hydrogen blends over a range of volume fractions of hydrogen. The modeling results from two alternative turbulence models such as k- $\Omega$  models and k- $\Omega$  SST models show no significant differences (Table 2).

### Results and discussion

In order to operationalize hydrogen blending in natural gas networks, it is important to fully understand the characteristics of the flow behavior of gas blends as they are transported across the transmission, distribution, and household sections of the pipeline infrastructure. As the gas blends are transported across several sections of the gas networks, they are expected to encounter different materials such as cast iron, steel or polyethylene (PE) with their characteristic surface roughness, different pipe diameters and also pipe bends. CFD models are developed to characterize the influence of pipe roughness, pipe diameter and pipe bends on the flow behavior of methane-hydrogen gas blends and the energy costs associated with their transportation.

## Effect of pipe surface roughness

In order to obtain a comprehensive understanding of the effects of pipe surface roughness on the pressure drop characteristics and the energy costs associated with the transport of methane-hydrogen gas blends, CFD models were developed for three major pipe materials with their characteristic surface roughness, under three gas flow boundary conditions, i.e., constant mass flow rate, constant inlet volumetric flow rate, constant energy flow rate, for six methane/hydrogen

Table 2 — Comparison of results obtained from the CFD models for methane-10 vol% hydrogen blend of Cadorin et al. [32] with those of the present study (Reference case) using  $k-\epsilon$ ,  $k-\Omega$  and SST models for turbulence. A comparison of the CFD models by Cadorin et al., the present study (Model case  $k-\epsilon$ ) for the flow of natural gas (NG) with the experimental results are also presented.

		Cadorin et al. (10%H <sub>2</sub> )	Reference Case $k-\epsilon$ (10% $H_2$ )	Reference Case $k-\Omega$ (10% $H_2$ )	Reference Case SST (10% H <sub>2</sub> )	Cadorin et al. (NG)	Model Case k-ε (NG)	Experimental Data (NG)
ṁ	[kg/s]	32.6	32.6	32.6	32.6	32.6	32.6	31.8
р	[kPa]	6000	6000	6000	6000	6000	6000	6718
T	[K]	303.15	303.15	303.15	303.15	303.15	303.15	309.1
ρ	$[kg/m^3]$	39.3	38.5	38.4	38.2	55.6	55.6	58.12
μ	[Pa s]	$1.33 \times 10^{-5}$	$1.22 \times 10^{-5}$ [9]	$1.22\times10^{-5}$	$1.22\times10^{-5}$	$1.38\times10^{-5}$	$1.38\times10^{-5}$	$1.27\times10^{-5}$
LHV	[KJ/kg]	49,258	50,910	50,910	50,910	47,351	47,351	_
Re	[-]	$2.09 \times 10^{7}$	$2.31 \times 10^{7}$	$2.30 \times 10^{7}$	$2.29 \times 10^{7}$	$2.00 \times 10^7$	$2.01 \times 10^7$	$2.00 \times 10^{7}$
Δр	[kPa]	22.1	22.3	22.8	23.3	15.5	15.7	_
L	[m]	4	4	4	4	4	4	_
$f_N$	[-]	$1.91\times10^{-2}$	$1.89 \times 10^{-2}$	$1.93\times10^{-2}$	$1.96\times10^{-2}$	$1.90\times10^{-2}$	$1.92\times10^{-2}$	$2.05\times10^{-2}$
EST	$[m^{-1}]$	$2.86 \times 10^{-6}$	$2.84 \times 10^{-6}$	$2.92 \times 10^{-6}$	$2.99 \times 10^{-6}$	$1.47 \times 10^{-6}$	$1.49 \times 10^{-6}$	_

Table 3 — Boundary conditions used for CFD simulations to assess the effect of surface roughness [15,38].					
		Flow Boundary Conditions			
		Constant mass flow rate	Constant inlet velocity	Constant energy flow rate	
Pipe Material (Surface Roughness)	Cast iron (259 µm)	32.6 kg/s	48.8 m/s	1631630 kJ/s	
	Steel (50 µm)	32.6 kg/s	48.8 m/s	1631630 kJ/s	
	PE (5 μm)	32.6 kg/s	48.8 m/s	1631630 kJ/s	

concentrations (i.e., 100/0, 90/10, 75/25, 50/50, 25/75, 0/100) as summarized in Table 3. All the 54 CFD models were constructed using the same 6 m pipe section geometry with 150 mm inner diameter as illustrated in Fig. 1.

Upon determining the pressure drops associated with the transport of methane-hydrogen gas blends, the corresponding energy costs (as captured by the energy specific toll (EST)) were quantified for all the 54 models and are presented in Figs. 2 and 3.

In Fig. 2, the effects of the blended gas flow conditions on the energy costs for transporting gas blends are presented for each pipe material. CFD results indicate that the general trends observed in the energy cost required for transportation of methane-hydrogen gas blends with varying concentrations of hydrogen are similar for the transportation of gas blends across different materials. An increase in the energy costs is expected when hydrogen is transported along with methane in different blend ratios. The amount of increase in energy costs depends on the volume fraction of hydrogen and the nature of the flow conditions. The highest and lowest energy costs for gas transportation is expected for the case of pure hydrogen depending on different operating conditions.

The energy cost for transporting gases (i.e., the EST value) depends on three parameters —pressure drop, density and the LHV value of the gas. So, the overall variation of EST with respect to hydrogen content in the blends, depends on the variation of all these three parameters. Amongst these three parameters, the variation of pressure drop with hydrogen content in the blends, depends on the flow condition, i.e., constant velocity flow rate, constant mass flow rate or constant energy flow rate. For example, under constant velocity flow conditions and constant energy flow rate conditions, the pressure drop for transporting 100% hydrogen is less than that

for transporting 75%–25% hydrogen-methane blend which results in the EST value for the transport of 100% hydrogen being less than that of the blend with 75% hydrogen. On the other hand, under constant mass flow rate condition, the pressure drop for transporting 100% hydrogen is more than that for transporting 75%–25% hydrogen-methane blend, resulting in higher EST value for transporting 100% hydrogen.

In Fig. 3, the effects of the pipeline material (with different surface roughness) on the energy costs for transporting gas blends are presented for each of the three blended gas flow conditions. By directly comparing the energy costs associated with the transport of gas blends for different pipe materials, it is clearly observed that transportation in cast iron which has the highest surface roughness will incur the highest cost. The energy cost differential between transporting gas blends in cast iron and other pipeline materials increases as the hydrogen concentration increases in the gas mixtures, except in the case of pure hydrogen transport under constant inlet velocity and energy flow rate conditions.

An understanding of the reasons for the high energy costs associated with the transport of hydrogen in pipeline materials with higher surface roughness can be obtained by examining the flow characteristics of the gas blends inside the pipes, esp., near the pipe wall.

For example, under constant mass flow rate condition, the velocity profiles that are developed in the cast iron pipelines during the flow of gas blends with varying concentrations of hydrogen are presented in Fig. 4. The velocity difference between the near wall region and the center region increases as more hydrogen is blended into the mixture. Starting from the 25% hydrogen velocity profile, a non-smooth transition is present at the region between 25 mm and 55 mm away from the center.

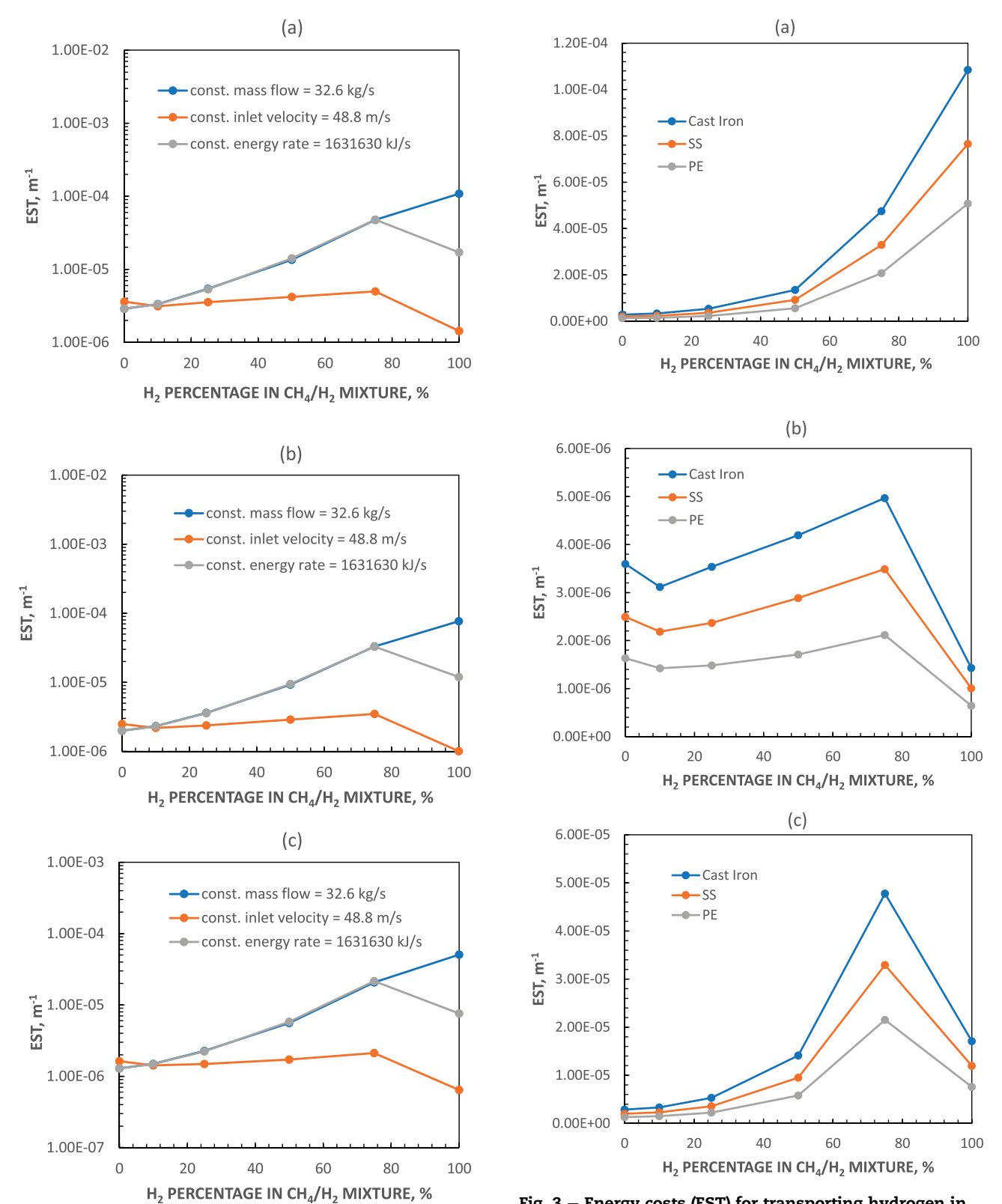


Fig. 2 — Energy costs (EST) for transporting hydrogen in methane-hydrogen mixtures in (a) Cast Iron; (b) Stainless Steel; (c) PE pipes.

Fig. 3 – Energy costs (EST) for transporting hydrogen in methane-hydrogen mixtures in (a) constant mass flow rate=32.6 kg/s; (b) constant inlet velocity=48.8 m/s; (c) constant energy rate=1631630 kJ/s.

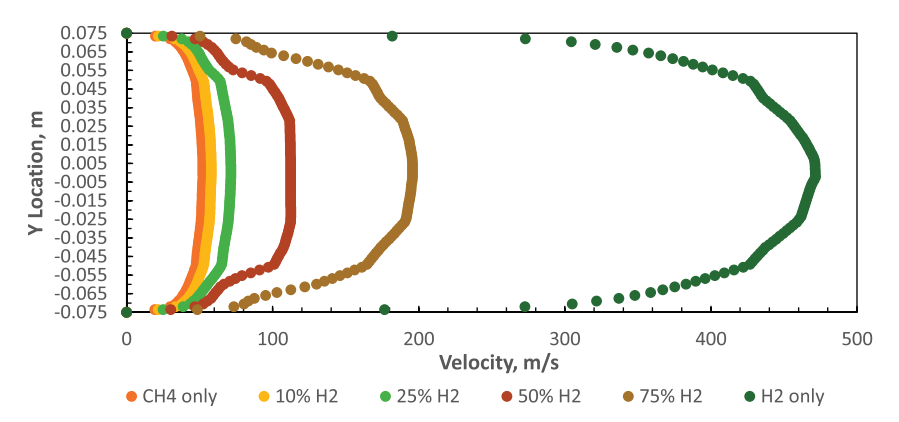


Fig. 4 — Velocity profiles of methane-hydrogen gas mixtures in a cast iron pipe with a constant mass flow rate=32.6 kg/s taken at 5 m away from the inlet.

The velocity profiles that are developed in pipelines of different materials for each blend concentration are mapped in Fig. 5. Comparing the gas velocities near the pipe walls across several gas blend concentrations, it is clear that pipelines with rougher surfaces like those present in the cast iron pipes have a greater effect on gas velocity reduction. Near the center of the pipe, smoother surface pipes such as PE pipes have the lowest velocity amongst three materials considered

in the present study. In general, as the hydrogen concentration increases in the methane-hydrogen mixture, the shape of the velocity profile turns sharper, which indicates a greater difference in the gas velocity between the near wall and center pipe locations, with the exception of the pure hydrogen case where the differences in the velocity profiles are reduced. While the velocity of the pure hydrogen gas is the highest in all the cases under constant mass flow rate conditions, the

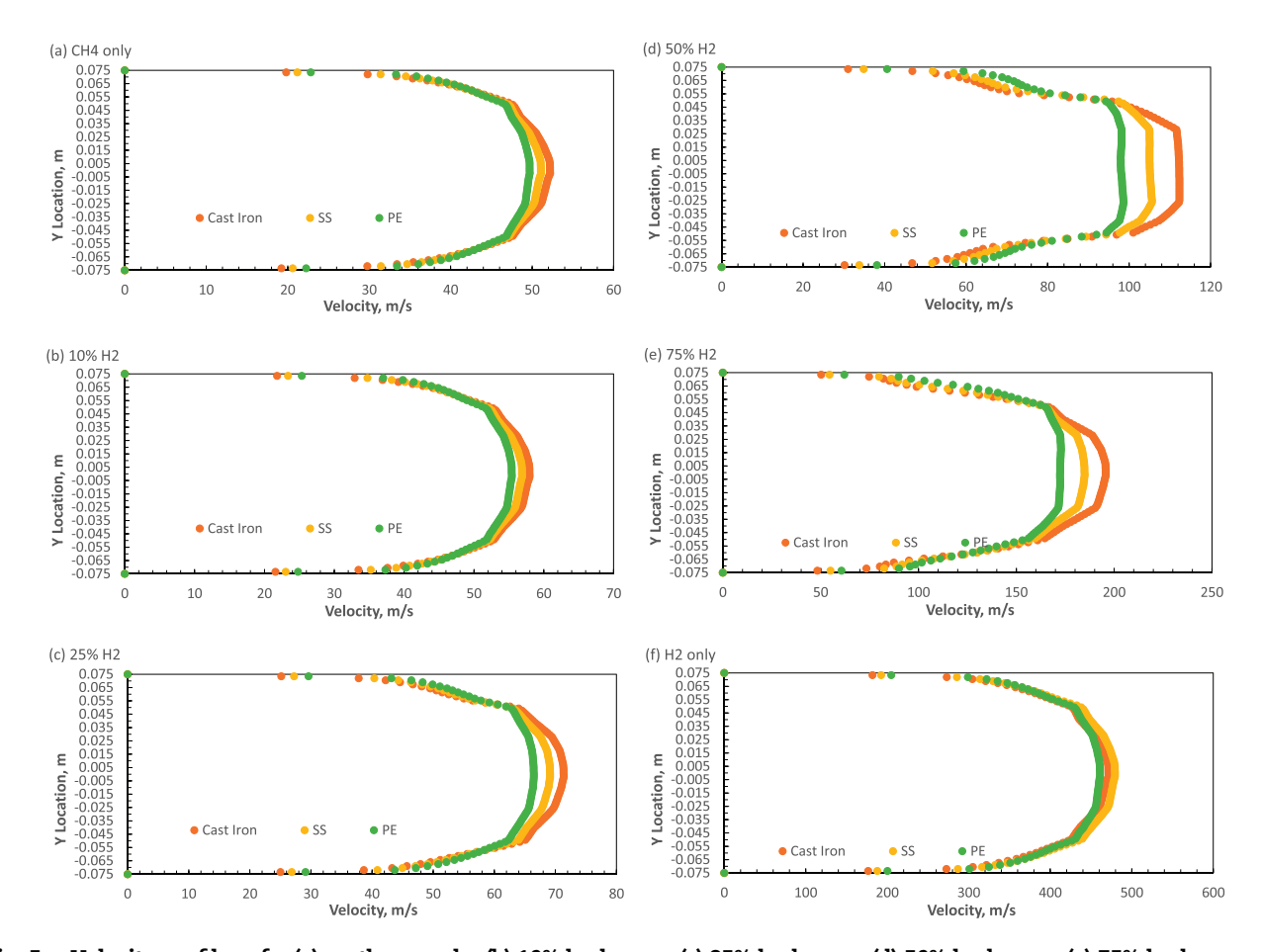


Fig. 5 — Velocity profiles of a (a) methane only; (b) 10% hydrogen; (c) 25% hydrogen; (d) 50% hydrogen; (e) 75% hydrogen; (f) hydrogen only methane-hydrogen gas mixture in pipes with a constant mass flow rate=32.6 kg/s taken at 5 m away from the inlet.

Table 4- The operating conditions for the CFD models developed for the transport of hydrogen blends across the distribution, transmission, and household pipelines with different diameters.

		Flow Boundary Conditions			
		Constant mass flow rate	Constant inlet velocity	Constant energy flow rate	
Pipe Type	Transmission Distribution Household	32.6 kg/s 32.6 kg/s	48.8 m/s 48.8 m/s 48.8 m/s	1631630 kJ/s 1631630 kJ/s	

velocity profile is relatively smooth between the near wall and the center locations of the pipe.

The velocity profiles of some methane-hydrogen blends (e.g., 25%–75% H2 case) show abrupt transitions between the near wall region and the center pipe region. It is hypothesized that the uneven mixing of hydrogen and methane gases is the main reason behind it. As presented in a later section 3.4, gases of different densities can separate during flow, which can affect the final velocity profile of the gas mixture.

### Effect of pipe diameter

In order to obtain a comprehensive understanding of the effects of pipe diameter on the pressure drop characteristics and the energy costs associated with the transport of methanehydrogen gas blends, across the transmission, distribution and household pipelines, 42 CFD models were developed for three pipe sections with their characteristic diameters, under three gas flow boundary conditions, i.e., constant mass flow rate, constant inlet volumetric flow rate, constant energy flow rate, for six methane/hydrogen concentrations (i.e., 100/0, 90/10, 75/25, 50/50, 25/75, 0/100) as summarized in Table 4. The pipe surface roughness was maintained at 50  $\mu m$ . The sizes of the pipe models and their corresponding operating pressures are listed in Table 5. The mesh controls for the modeled pipe sections are presented in Table 6.

In order to assess the energy costs associated with the transport of methane-hydrogen gas blends in transmission pipelines, the pressure drop results are taken from the last

Table 5 — Pipe sizes and operating conditions invoked in the GFD models developed for understanding the effects of pipe diameter.

Pipe Type	Pipe ID, mm	Pipe Length, m	Operating Pressure, kPa
Distribution	150	6	6000
Transmission	483	20	10,340
Household	14	0.6	1.38

# Table 6 – Mesh controls used in the CFD models developed for understanding the effects of pipe diameter.

Pipe Type	Element Size, mm	Number of Elements	Number of Inflation Layers	Inflation Layer Total Thickness, mm
Distribution	12	476,965	7	25
Transmission	39	484,027	7	80
Household	1.15	487,363	7	2.3

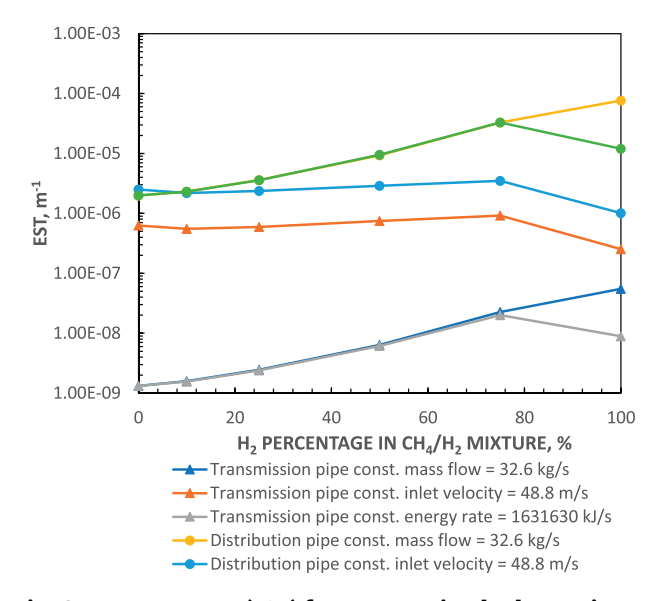


Fig. 6 – Energy costs (EST) for transporting hydrogen in methane-hydrogen mixtures in  $6^{\prime\prime}$  distribution pipes and  $20^{\prime\prime}$  transmission pipes.

14 m of the pipe to avoid the unestablished flow domain near the inlet section.

In Fig. 6, the energy costs for transporting gas blends in the larger transmission pipelines (with 20 inch diameter) are compared to the costs associated with transporting gas blends in smaller distribution lines (with 6 inch diameter). It is found that, in general, it costs less energy to transport gas blends in the larger transmission pipelines as compared to the smaller distribution lines for all the three gas flow conditions considered in this study. Amongst all the cases, the transport of gases under conditions of constant mass flow rate and constant energy flow rate requires the least energy penalty. The energy costs for transporting gas blends in the distribution lines are about four times more than that for transporting gases in transmission lines under identical inlet velocity conditions.

In the household pipe model, the pressure drop results are taken from the last 0.4 m of the pipe to avoid the unestablished flow domain near the inlet section.

A constant inlet velocity has been applied in the household pipe models only due to the size and the operating conditions of the pipe in real life. The Reynolds numbers calculated from the velocity results suggest that laminar flows are observed which is also observed in the CFD simulations.

Comparing the energy required for transporting gas blends between the distribution pipelines (with 6 inch diameter) and household pipelines (with 0.5 inch diameter), it is evident that more energy is required to transport gas blends in the smaller

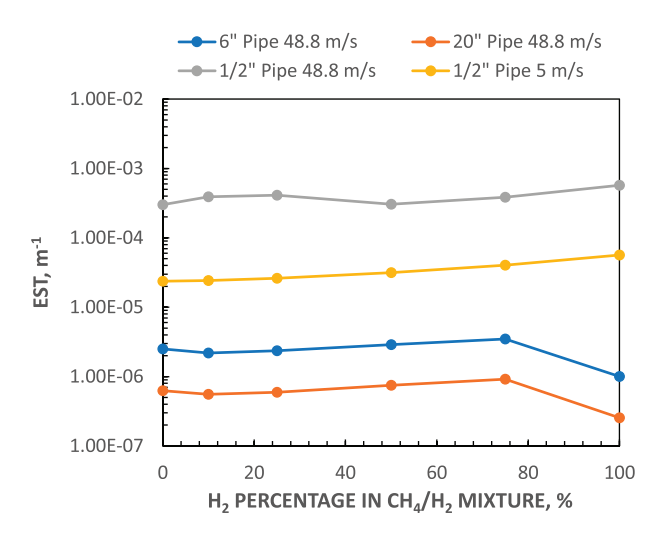


Fig. 7 – Energy costs (EST) for transporting hydrogen in methane-hydrogen mixtures at inlet velocities of 48.8 m/s and 5 m/s.

household pipes (Fig. 7). In the first analysis, the velocity of gas in the household pipelines is assumed to be the same as in the distribution lines. In the second analysis, the velocity is reduced to the range that is typically expected in the household pipes and proportionately [39], the energy costs are reduced as well.

### Effect of pipe bends

As pipe bends are an integral part of the gas networks, it is also important to assess the effect of pipe bends on the flow behavior of methane-hydrogen gas blends. In this study, CFD models were developed to understand the flow characteristics associated with a 90° pipe bend section of a distribution pipeline (with 150 mm inner diameter and 50  $\mu m$  surface roughness), under three distinct operating conditions (i.e., constant mass flow rate, constant inlet volumetric flow rate, constant energy flow rate) for several methane/hydrogen concentration ratios (i.e., 100/0, 90/10, 75/25, 50/50, 25/75, 0/100).

Fig. 8 demonstrates the geometry of the bending pipe section as well as the boundary conditions applied in the model.

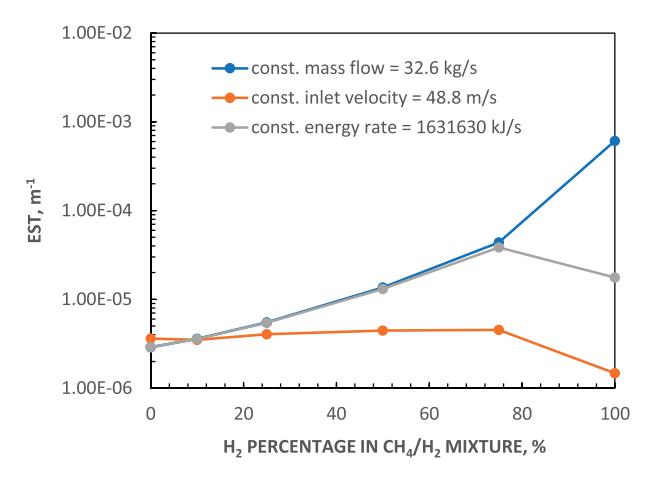


Fig. 9 – Energy costs (EST) for transporting hydrogen in methane-hydrogen mixtures in a 150 mm ID distribution pipe bend section.

In the distribution pipe bend model, the pressure drop results are taken from the last 2 m of the horizontal pipe section and the 2 m of the vertical pipe section to avoid the unestablished flow domain near the inlet section. A total of 475,927 mesh elements with average element size of 12 mm were utilized to build the geometry. Inflation was used to refine the near wall region of the mesh. A total of 7 inflation layers were included in the meshed geometry and total inflation layer thickness was 25 mm.

The energy costs associated with transporting methane-hydrogen gas blends across pipe bend sections are illustrated in Fig. 9. The trends observed for the transportation across straight pipe sections are observed here as well. Transporting pure hydrogen at a constant inlet velocity requires the lowest energy cost, while transporting pure hydrogen in the constant mass flow rate requires the highest energy cost.

A direct comparison is also made between the energy costs associated with the transport of gas blends in straight sections and bend sections of pipelines as illustrated in Fig. 10. It can be clearly observed that pipe bends will generally require higher energy costs for gas transport in all the three operating scenarios that are considered in this study. The energy cost gap

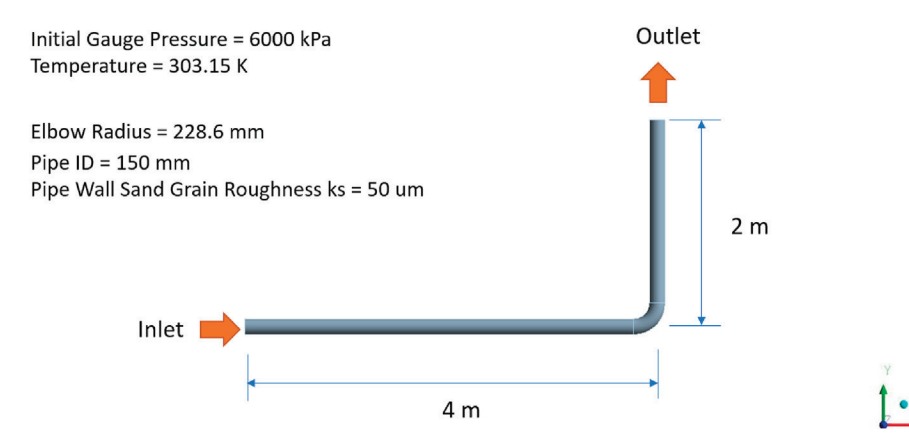


Fig. 8 – The geometry and boundary conditions used for modeling pipe bends.

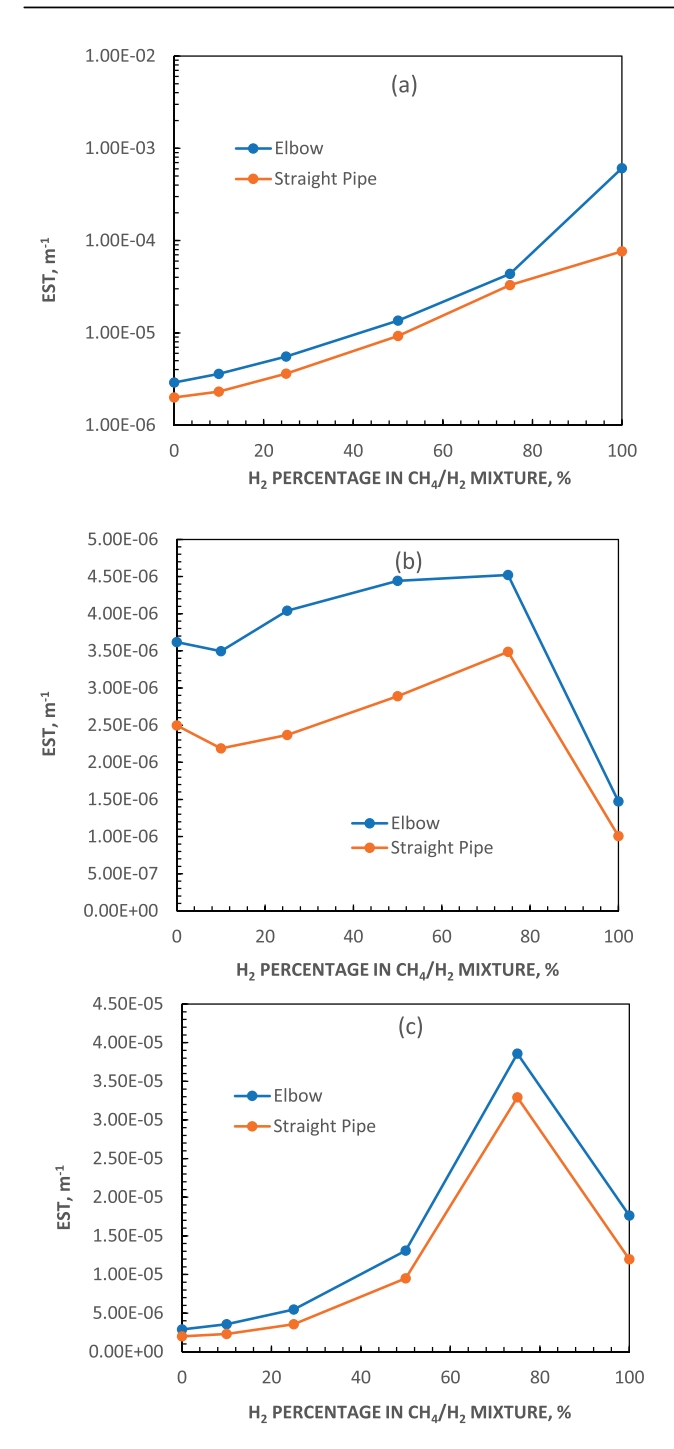


Fig. 10 — Energy costs (EST) for transporting hydrogen in methane-hydrogen mixtures in a 150 mm ID straight pipe section and a bending pipe section at (a) constant mass flow rate=32.6 kg/s; (b) constant inlet velocity=48.8 m/s; (c) constant energy rate=1631630 kJ/s.

between straight pipe section and bending pipe section is on average about 50% except in the case of pure hydrogen case at constant mass flow rate condition, in which case the energy cost gap is about 700%.

## Understanding the mixing behavior of methane-hydrogen gas blends

The evolution of the mixing behavior of methane-hydrogen gas blends was evaluated with several CFD models. All these models were constructed with a pipe with 150 mm inner diameter with 50  $\mu$ m inner surface roughness. Six concentrations of hydrogen were considered with a constant mass rate of 32.6 kg/s.

Fig. 11 demonstrates the steady state distribution of hydrogen in the pipe model from 10% to 75% hydrogen concentration in the transporting gas mixture. At the 5 m, 10 m, and 16 m mark of the pipe, the hydrogen distribution is captured by noting the corresponding volume fractions of hydrogen in the pipeline cross-sections.

From the hydrogen volume fraction contours extracted in each concentration load case, it is observed that methane, the denser and more viscous gas component, is concentrated mostly in the near wall region of the pipe, while the lighter and less viscous hydrogen species is found mostly grouped in the center of the pipe and surrounded by the methane.

In order to fully understand the rationale for this pattern of heterogeneous gas separation, even under turbulent flow conditions, a second set of CDF models was constructed where in methane was replaced with the denser argon to simulate the flow of argon-hydrogen mixtures for the same pipe geometry and flow boundary conditions used in the methane-hydrogen case. Fig. 12 demonstrates the hydrogen volume fraction contours of the 18-m pipe section at constant mass flow rate=32.6 kg/s running an argon-hydrogen mixture. At 5 m, 10 m, and 16 m mark of the pipe, hydrogen volume fraction results of the corresponding cross-section are displayed on top of the overall pipe section.

The gas distribution in this set of models also show a very similar pattern when compared to the results of the methane-hydrogen mixture models. It is noted that even under turbulent flow conditions in a round pipe, gases of different densities are not well mixed. Lighter gases in the turbulent flow are surrounded by the denser gases across the axial direction of the pipe section.

From the CFD models on methane-hydrogen and argonhydrogen gas blends, it is evident that a non-mixed flow pattern develops in the pipelines. While the overall Reynolds number for the flow indicates that the flow is occurring under turbulent conditions, it is noted that turbulence is not an effective mixer in the methane-hydrogen blends transported across pipelines, with neither axial mixing nor turbulent mixing being observed in the volume fraction contours. The observed core-annular flow pattern in the gas blends with more than 50% hydrogen is similar to that found in some liquid-liquid flows. Hydrogen, the less viscous gas flows in the core, while the more viscous gas methane flows in the annulus.

While there are few reports of such heterogeneous mixing in binary gases, the occurrence of such core-annular flow patterns has been noted and analyzed in the case of binary liquids. In the binary liquid systems, it was found that the

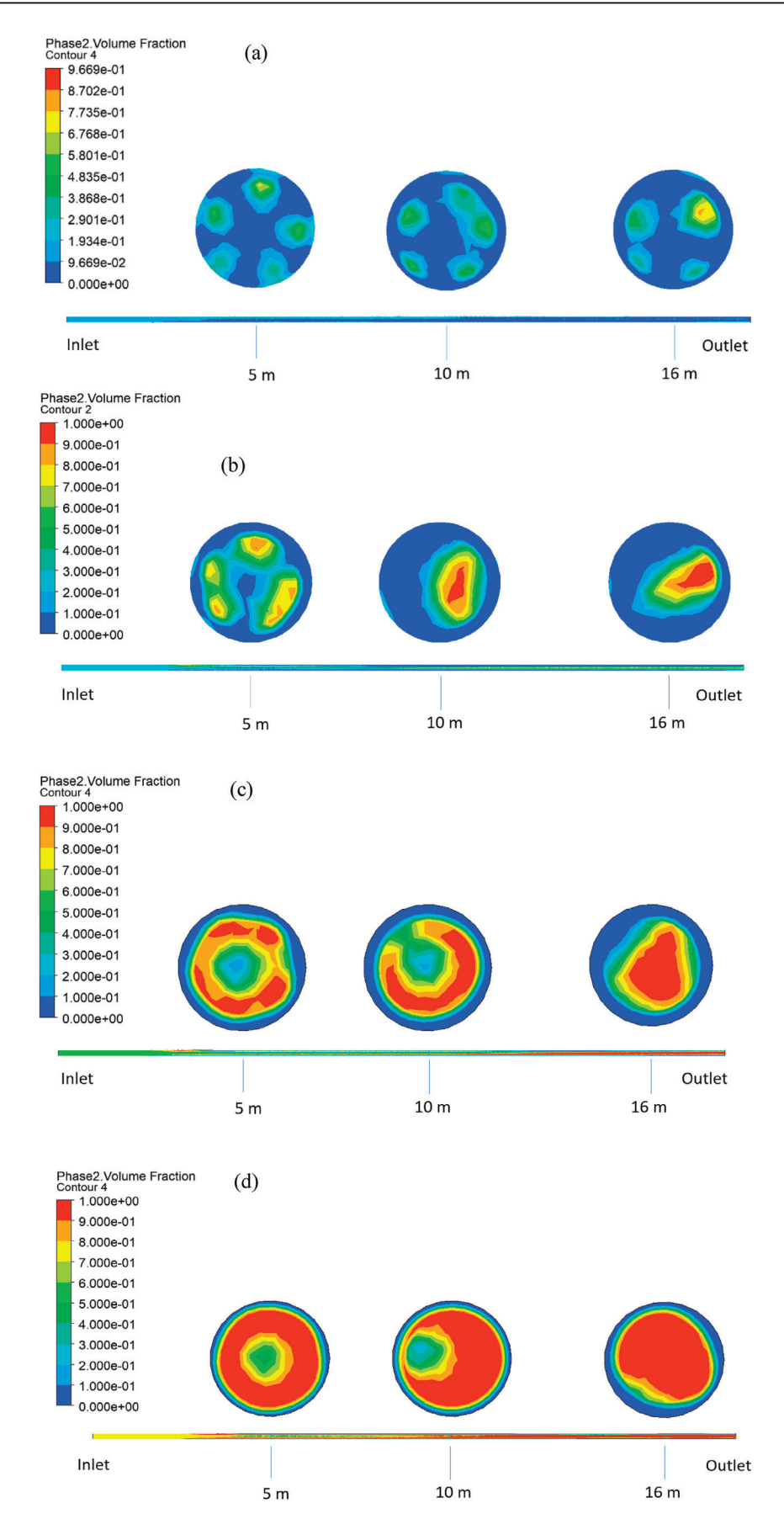


Fig. 11 — Hydrogen (phase 2) volume fraction profile in a 150 mm ID by 18 m long stainless steel pipe transporting methanehydrogen mixtures: (a) 10%; (b) 25%; (c) 50%; (d) 75% hydrogen.

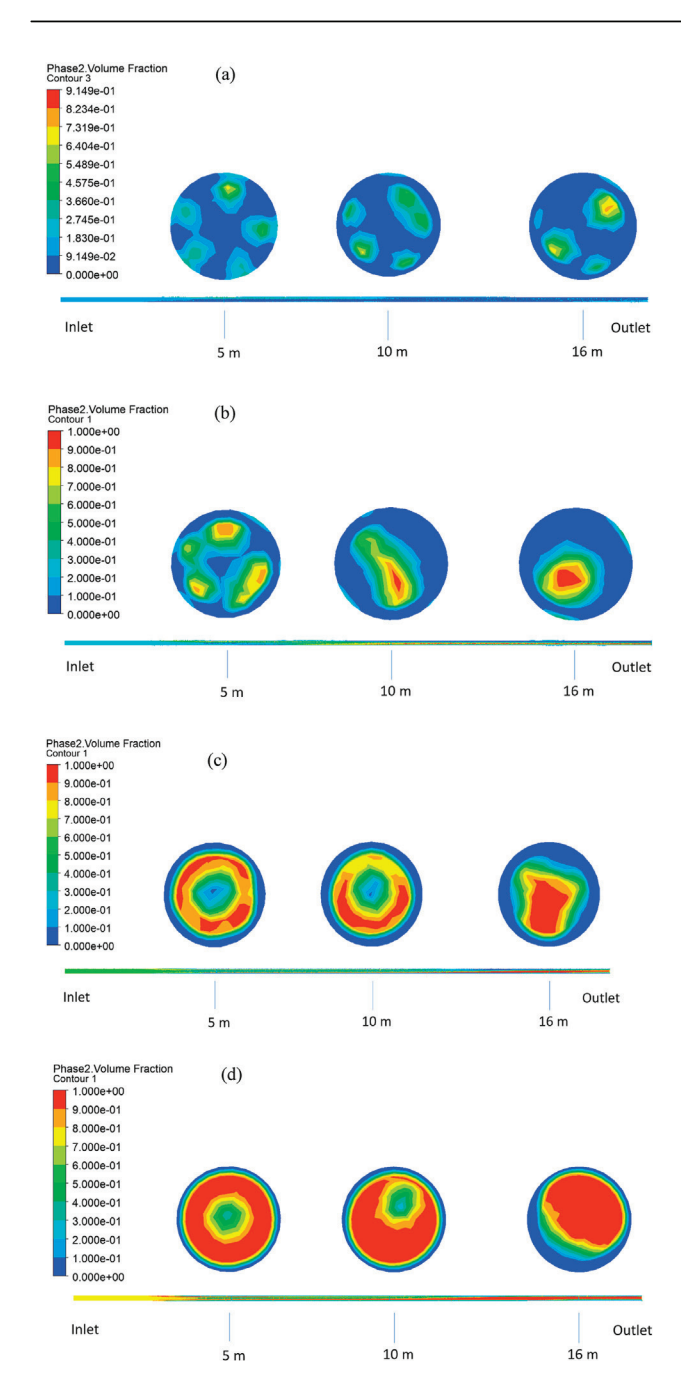


Fig. 12 — Hydrogen (phase 2) volume fraction profile in a 150 mm ID by 18 m long stainless steel pipe transporting argon-hydrogen mixtures: (a) 10%; (b) 25%; (c) 50%; (d) 75% hydrogen.

gravitation to viscous force ratio (G/V) governs the mixing behavior and flow pattern. Core-annular flow was typically observed in systems with a low G/V ratio (less than 140) [40]. The absolute values of the G/V ratios in the methanehydrogen binary gas system considered in this study (4600–11300) are much higher than those observed in the liquid-liquid system due to the much lower viscosity values of the gases. However, as the hydrogen concentration is increased in the methane-hydrogen gas blends, the G/V value is reduced which correlates with the observation that the core-annular flow pattern is more prominent in gas blends

with higher hydrogen concentrations. Thus, the trends observed in the mixing behavior of binary gases are similar to those that have been observed in binary liquids.

In addition to enhancing the fundamental understanding of the flow characteristics of the methane-hydrogen gas blends, it is expected that the observed mixing characteristics will also impact strategies for potential gas separation applications near the end-use locations in gas networks as well.

### Conclusions

Replacing fossil fuels and natural gas with alternative fuels like hydrogen is an important strategy towards realizing a carbon neutral economy. As an intermediate step towards ultimately utilizing pure hydrogen, blending hydrogen in an existing natural gas network is a potential pathway for reducing carbon emissions. Prior studies have shown that transporting methane-hydrogen gas blends would require additional energy to compensate for the increased pressure losses expected due to the introduction of hydrogen. However, a comprehensive study of the cost of transporting methanehydrogen gas blends across various parts of the pipeline infrastructure such as transmission, distribution and household pipelines that takes into consideration the variations of pipe surface roughness and the effects of pipe bends is not yet available. Furthermore, characteristics of the mixing behavior of hydrogen in methane gas blends have not been investigated in detail as well.

Hence, a computational fluid dynamic (CFD) modeling framework was developed to quantify frictional losses and energy efficiency of transport of methane-hydrogen blends across representative sections of a large gas network. The following conclusions were obtained.

- While, in general, an increase in the energy costs is expected when hydrogen, with its lower density, is transported along with methane (which has higher density) in various blend ratios, the amount of increase in energy costs depends on the volume fraction of hydrogen, the nature of the flow conditions, pipe diameter, pipe roughness and pipe bends.
- 2. Pipelines that typically have larger surface roughness (such as cast iron) require greater energy for transporting gas blends due to the higher surface frictional effects compared to those that have lower surface roughness (such as steels and polyethylene). This observation suggests that careful surface finishing of pipelines would be very helpful towards mitigating the costs of hydrogen gas transport.
- 3. Pipelines with larger diameters are relatively more energy efficient than those with smaller diameters in transporting hydrogen. This observation is directly related to the lower surface area to the volume ratio of the larger pipes which reduces the frictional drag associated with the inner surface of the pipes. Thus, transporting methane-hydrogen gas blends in relatively larger diameter pipes, where practical, would help in enhancing the efficiency of the transportation of methane-hydrogen gas blends.

- 4. Pipeline bend sections also introduce an additional energy penalty for the transportation of methane-hydrogen gas blends. Thus, minimizing pipe bends, where possible, in designing the hydrogen gas networks would help alleviate the energy costs associated with the transport of hydrogen.
- 5. The methane-hydrogen gas blends tend to develop a coreannular flow pattern under steady state conditions with the denser and more viscous methane flowing near the pipe wall as the annulus while the less dense and less viscous hydrogen concentrated more towards the midsections of the pipelines. Thus, turbulence is an inefficient mixer in the case of methane-hydrogen gas blends in the flow conditions considered in this study with implications for the development of gas separation technologies near the end-use application locations.

## **Declaration of competing interest**

The authors declare that they have no known competing financial interests or personal relationships that could have appeared to influence the work reported in this paper.

## **Acknowledgements**

This research was funded by the NSF DMREF grant #2119337 and NYSERDA grant# 148947.

#### **Nomenclature**

time

temperature

inlet velocity

t

T

Α	area
С	constant
D	diameter
Ė	energy transport rate
F	external body force
f	Moody frictional factor
$f_N$	numerical friction factor
g	gravitational acceleration
$G_b$	generation of turbulence kinetic energy due to
	buoyancy
$G_k$	generation of turbulence kinetic energy due to mean
	velocity gradients
$h_{\rm L}$	frictional head loss
I	unit tensor
k	turbulence kinetic energy
ks	sand grain roughness
L	length
m	mass flow rate
$\dot{m}_{pq}$	mass transferred from phase p to phase q
$\dot{m}_{qp}$	mass transferred from phase q to phase p
p	pressure
Re	Reynolds number
S	source term

U	average now velocity
V	volume
X	displacement
$Y_M$	the contribution of the fluctuating dilatation
$\alpha_q$	volume fraction of qth fluid
$\epsilon$	rate of dissipation in Equation (6) or empirical pipe
	roughness in Equation 11 and 12
$\sigma$	Prandtl numbers
$\rho$	gas or fluid density
$egin{pmatrix}  ho \ = \  au \end{matrix}$	stress tensor
$\mu$	viscosity

average flow velocity

#### REFERENCES

- [1] Gondal IA. Hydrogen integration in power-to-gas networks. Int J Hydrogen Energy 2019;44:1803—15.
- [2] Dias V, Pochet M, Contino F, Jeanmart H. Energy and economic costs of chemical storage. Front Mech Eng 2020:6:21
- [3] Flekiewicz M, Kubica G. An influence of methane/hydrogen proportion in fuel blend on efficiency of conversion energy in SI engine. J KONES 2012;19:117–24.
- [4] Mariani A, Unich A, Minale M. Combustion of hydrogen enriched methane and biogases containing hydrogen in a controlled auto-ignition engine. Appl Sci 2018;8:2667.
- [5] Obanijesu EO, Barifcani A, Pareek VK, Tade MO. Experimental study on feasibility of H2 and N2 as hydrate inhibitors in natural gas pipelines. J Chem Eng Data 2014;59:3756–66.
- [6] Mahajan D, Tan K, Venkatesh TA, Kileti P, Clayton CR. Hydrogen blending in gas pipeline networks – a review. Energies 2022;15:3582.
- [7] Isaac T. HyDeploy: the UK's first hydrogen blending deployment project. Clean Energy 2019;3(2):114–25.
- [8] GRHYD, https://www.engie.com/en/businesses/gas/ hydrogen/power-to-gas/the-grhyd-demonstration-project;
- [9] Blanchard L, Briottet L. Non-combustion related impact of hydrogen admixture – material compatibility. THyGA Project; 2020.
- [10] NREL. https://www.nrel.gov/news/program/2020/hyblend-project-to-accelerate-potential-for-blending-hydrogen-in-natural-gas-pipelines.html; 2020.
- [11] Lowesmith BJ, Hankinson G, Spataru C, Stobbart M. Gas build-up in a domestic property following releases of methane/hydrogen mixtures. Int J Hydrogen Energy 2009;34:5932—9.
- [12] Kobayashi Y, Kurokawa A, Hirata M. Viscosity measurement of hydrogen-methane mixed gas for future energy systems. J Therm Sci Technol 2008;2:236—44.
- [13] Fokin LR, Kalashnikov AN, Zolotukhina AF. Transport properties of mixtures of rarefied gases. Hydrogen-methane system. J Eng Phys Thermophys 2011;84:1408–20.
- [14] Chuang SY, Chappelear PS, Kobayahsi R. Viscosity of methane, hydrogen, and four mixtures of methane and hydrogen from -100C to 0C at high pressures. J Chem Eng Data 1976;21:403—11.
- [15] Perry RH, Green DW. Perry's chemical engineers' handbook. 7<sup>th</sup> ed. MCGRAW-HILL; 1997. p. 631.
- [16] Glanville P, Fridlyand A, Sutherland B, Liszka M, Zhao Y, Bingham L, Jorgensen K. Impact of hydrogen/natural gas blends on partially premixed combustion equipment: NOx emission and operational performance. Energies 2022;15:1706.

## ARTICLE IN PRESS

- [17] Zhao Y, McDonell V, Samuelsen S. Experimental assessment of the combustion performance of an oven burner operated on pipeline natural gas mixed with hydrogen. Int J Hydrogen Energy 2019;44:26049–62.
- [18] Shih H-Y, Liu C-R. A computational study on the combustion of hydrogen/methane blended fules for a micro gas turbines. Int J Hydrogen Energy 2014;39:14103-5115.
- [19] Wagner K, Tiwari P, Swiegers GF, Wallace GG. Alkaline fuel cells with novel gortex-based electrodes are powered remarkably efficiently by methane containing 5% hydrogen. Adv Energy Mater 2018;8:1702285.
- [20] Bainier F, Kurz R, Turbines S. Impact of H2 blending of capacity and efficiency on a gas transport network. Proceedings of the ASME Turbo Expo: Turbomachinergy Technical Conference and Exposition 2019;9.
- [21] Quintino FM, Nascimento N, Fernandes EC. Aspects of hydrogen and biomethane introduction in natural gas infrastructure and equipment. Hydro 2021;2:301–18.
- [22] Hafsi Z, Elaoud S, Akrout M, Hadj-Taieb E. Numerical approach for steady state analysis of hydrogen-natural gas mixture flows in looped network. Arabian J Sci Eng 2017;42:1941–50.
- [23] Liu J, Teng L, Han P, Li W. Analysis of hydrogen gas injection at various compositions in an existing natural gas pipeline. Front Energy Res 2021;9:685079.
- [24] Cavana M, Mazza A, Chicco G, Leone P. Electrical and gas networks coupling through hydrogen blending under increasing distributed photovoltaic generation. Appl Energy 2021;290:116764.
- [25] Fiebig C, Hielscher A, Span R, Gulin A, Rickelt S, Schley P. Gas quality tracking in distribution grids with SmartSimapplication in complex and smeshed grids. In: Proceedings of the international gas union research conference-IGRC; 2014. Copenhagen, Denmark, 17–19 September.
- [26] Dell'Isola M, Ficco G, Moretti L, Perna A, Candelaresi D, Spazzafumo G. Impact of hydrogen injection on thermophysical properties and measurement reliability in natural gas network. E3S Web Conf 2021;312:01004.
- [27] Umuteme OM. Computational fluid dynamics (CFD) transient pressure and temperature simulation of a natural gas-hydrogen gas blend transportation pipeline.

- International Journal of Innovative Research and Development 2020;9(6):112–6.
- [28] Liu B, Liu X, Lu C, Godbole A, Michal G, Teng L.

  Decompression of hydrogen-natural gas mixtures in highpressure pipelines: CFD modelling using different equations
  of state. Int J Hydrogen Energy 2019;44:7428—37.
- [29] Kuczynski S, Laciak M, Olijnyk A, Szurlej A, Wlodek T. Thermodynamic and technical issues of hydrogen and methane-hydrogen mixtures pipeline transmission. Energies 2019;12:569.
- [30] Sulaiman SZ, Kasmani RM, Kiah MHM, Kidam K, Hassim MH, Ibrahim N, Ali RR. The influce of 90 degree bends in closed pipe system on the explosion properties using hydrogenenriched methane. Chemical Engineering Transactions 2014;36:271–6.
- [31] Wilkening H, Baraldi D. CFD modelling of accidental hydrogen release from pipelines. Int J Hydrogen Energy 2007;32(13):2206–15.
- [32] Cadorin M, Morini M, Pinelli M. Numerical analyses of high Reynolds number flow of high pressure fuel gas through rough pipes. Int J Hydrogen Energy 2010;35:7568–79.
- [33] Tan K, Mahajan D, Venkatesh TA. Computational fluid dynamic modeling of methane-hydrogen mixture transportation in pipelines: estimating energy costs. MRS Advances 2022;7(19):388–93.
- [34] Tichacek LJ, Barkelew CH, Baron T. Axial mixing in pipes. AIChE J 1957;3(4):439–42.
- [35] Dimotakis PE. Turbulent mixing. Annu Rev Fluid Mech 2005;37:329–56.
- [36] Buaria D, Clay MP, Sreenivasan KR, Yeung PK. Turbulence is an ineffective mixer when Schmidt numbers are large. Phys Rev Lett 2021;126:074501.
- [37] Schlichting H. Experimental investigation of the problem of surface roughness. Ing Arch 1937;7(1).
- [38] NORSOK standard P-001. 5<sup>th</sup> ed. 2006. https://www.standard. no/en/sectors/energi-og-klima/petroleum/norsok-standard-categories/p-process/p-0012/.
- [39] Gas pipe line calculation sizing. 2013. https://www.edcgov.us/Government/building/documents/Gas%20Pipe%20Sizing%20%28Natural%29.pdf.
- [40] Shi J, Yeung H. Characterization of liquid-liquid flows in horizontal pipes. AIChE J 2017;63(3):1132–43.